Mathematical Modeling of Cation Contamination in a Proton-exchange Membrane

Adam Z. Weber[**] and Charles Delacourt[*]

Lawrence Berkeley National Laboratory, 1 Cyclotron Road, Berkeley CA 94720, USA

Transport phenomena in an ion-exchange membrane containing both H^+ and K^+ are described using multicomponent diffusion equations (Stefan-Maxwell). A model is developed for transport through a Nafion 112 membrane in a hydrogen-pump setup. The model results are analyzed to quantify the impact of cation contamination on cell potential. It is shown that limiting current densities can result due to a decrease in proton concentration caused by the build-up of contaminant ions. An average cation concentration of 30 to 40 % is required for appreciable effects to be noticed under typical steady-state operating conditions.

**Corresponding author, azweber@lbl.gov, 510-486-6308

*Current address: Laboratoire de Réactivité et Chimie des Solides, Université de Picardie Jules Verne, 33 Rue St Leu, 80039 Amiens cedex, France

Keywords: ion-exchange membrane, Nafion, contamination, mathematical model, Stefan-Maxwell equations, multicomponent diffusion equations, hydrogen pump

1. Introduction

Proton-exchange membranes are the current electrolyte of choice for polymer-electrolyte fuel cells (PEFCs). They have the key properties of being conductive to protons but not allowing gas permeation and have good durability and mechanical properties. However, these polymers can be susceptible to various contaminate ions. Examples of such ions include those arising from environmental conditions (*e.g.*, potassium and sodium from various salts)[1, 2] or cell operation (*e.g.*, dissolved platinum catalysts or iron from the bipolar plates)[3, 4]. While the latter has been investigated in various capacities, the former has not received much attention.[1, 2, 5]

The most complete theoretical study of the cation-contaminant effect in a PEFC environment was conducted by Kienitz *et al.*,[5] using a dilute-solution approach for the modeling. In this paper, we use a more rigorous model based on the Stefan-Maxwell multicomponent equations to study the impact of potassium ions on the steady-state performance of a hydrogen pump, where there is humidified hydrogen on the anode side of the membrane and humidified nitrogen on the cathode side. The simplified example of a hydrogen pump allows one to focus on the cation-contaminant impact without interference from other fuel-cell inefficiencies such as the concentration overpotentials, the sluggish oxygen-reduction-reaction kinetics, as well as water-management issues. By examining the limiting currents that result due solely to proton conduction and concentration, one can gain insight into how the overall cell performance would be affected. It should be noted that in this paper the membrane is treated as a separator. While the impact of contaminant ions of the dispersed ionomer in the catalyst layers can be related to the discussion below, additional factors such as the need for gas permeation and the thinness of ionomeric films make a detailed modeling study of the catalyst layer beyond the scope of this paper.

2. Theory

Governing Equations— For the problem, there are eight unknowns that must be solved for: the mole fractions for proton, potassium cation, water, and membrane, x_{H^+}, x_{K^+}, x_{H_2O}, and x_{M^-}, respectively, the flux densities, N_{H^+}, N_{K^+}, N_{H_2O}, and the potential in the membrane, Φ_2. The flux of membrane, N_{M^-}, is set to zero, as is appropriate in a steady state. Eight equations are thus required.

As mentioned in the introduction, concentrated solution theory is used for the system under consideration. For an isothermal system composed of two cations, water, and membrane, there are three independent Stefan-Maxwell equations[6-8]

$$c_{H^+}\nabla\mu_{H^+} = RT\left(\frac{x_{H^+}\mathbf{N}_{H_2O} - x_{H_2O}\mathbf{N}_{H^+}}{\mathcal{D}_{H^+,H_2O}} + \frac{-x_{M^-}\mathbf{N}_{H^+}}{\mathcal{D}_{H^+,M^-}} + \frac{x_{H^+}\mathbf{N}_{K^+} - x_{K^+}\mathbf{N}_{H^+}}{\mathcal{D}_{H^+,K^+}}\right) \tag{1}$$

$$c_{K^+}\nabla\mu_{K^+} = RT\left(\frac{x_{K^+}\mathbf{N}_{H_2O} - x_{H_2O}\mathbf{N}_{K^+}}{\mathcal{D}_{K^+,H_2O}} + \frac{-x_{M^-}\mathbf{N}_{K^+}}{\mathcal{D}_{K^+,M^-}} + \frac{x_{K^+}\mathbf{N}_{H^+} - x_{H^+}\mathbf{N}_{K^+}}{\mathcal{D}_{K^+,H^+}}\right) \tag{2}$$

and

$$c_{H_2O}\nabla\mu_{H_2O} = RT\left(\frac{x_{H_2O}\mathbf{N}_{H^+} - x_{H^+}\mathbf{N}_{H_2O}}{\mathcal{D}_{H_2O,H^+}} + \frac{-x_{M^-}\mathbf{N}_{H_2O}}{\mathcal{D}_{H_2O,M^-}} + \frac{x_{H_2O}\mathbf{N}_{K^+} - x_{K^+}\mathbf{N}_{H_2O}}{\mathcal{D}_{H_2O,K^+}}\right) \tag{3}$$

respectively, where $\mathcal{D}_{ij}$ are binary interaction coefficients between species *i* and *j* (which contain the macroscopic transport properties of ionic conductivity, electro-osmotic coefficient, proton transference number, and water permeability) and the other variables are as defined in the nomenclature. In the above equations, one needs to express the electrochemical potential of the four species. To do this, one defines the membrane potential with respect to a hypothetical hydrogen reference electrode,

$$\nabla\mu_{H^+} = F\nabla\Phi_2 \tag{4}$$

Note that a problem may arise in this particular system composed of two cations if the proton concentration goes to zero, in which case one would have to use another definition for the potential. Gradients of electrochemical potentials of the other ionic species are deduced from equation 4,

$$\nabla\mu_{K^+} = RT\left(\frac{\nabla x_{K^+}}{x_{K^+}} - \frac{\nabla x_{H^+}}{x_{H^+}}\right) + b\left(\nabla\left(y_{HM}{}^2\right) - \nabla\left(y_{KM}{}^2\right)\right) + F\nabla\Phi_2 \tag{5}$$

$$\nabla\mu_{M^-} = RT\left(\frac{\nabla x_{H^+}}{x_{H^+}} + \frac{\nabla x_{M^-}}{x_{M^-}}\right) + b\nabla\left(y_{KM}{}^2\right) - F\nabla\Phi_2 \tag{6}$$

and

$$\nabla\mu_{H_2O} = RT\frac{\nabla x_{H_2O}}{x_{H_2O}} \tag{7}$$

for potassium, membrane, and water, respectively. In the above derivations, pressure gradients are assumed to be of minimal importance. The following activity coefficients are considered [13]

$$f_{KM} = \exp\left(\frac{b}{RT}y_{HM}{}^2\right) \tag{8}$$

and

$$f_{HM} = \exp\left(\frac{b}{RT}y_{KM}{}^2\right) \tag{9}$$

where

$$y_{HM} = \frac{x_{H^+}}{x_{H^+} + x_{K^+}} \tag{10}$$

and

$$y_{KM} = \frac{x_{K^+}}{x_{H^+} + x_{K^+}} \tag{11}$$

Expression for these activity coefficients are derived by considering that the membrane behaves as a regular mixture of HM and KM. b is a constant taken equal to −151 J/mol [10]. As there are three unknown flux densities, one needs three material balances, which are of the form

$$\nabla \cdot \mathbf{N}_i = 0 \tag{12}$$

with i = H^+, K^+, and H_2O. The two remaining governing equations are the sum of the mole fractions,

$$x_{H^+} + x_{K^+} + x_{H_2O} + x_{M^-} = 1 \tag{13}$$

and electroneutrality,

$$x_{H^+} + x_{K^+} = x_{M^-} \tag{14}$$

To account for membrane swelling, two equations are added to the set of eight governing equations to be solved. Since the concentration of membrane can vary across the system but the thickness is constant, one solves for the thickness by using the equations[9]

$$\frac{\partial l}{\partial x} = 0 \tag{15}$$

and

$$\frac{\partial \eta}{\partial x} = c_{M^-} \tag{16}$$

where η is the total number of moles of membrane M^- per cross sectional area.

If one uses the Onsager reciprocal relations, $\mathcal{D}_{ij} = \mathcal{D}_{ji}$, then there are six binary interaction parameters that must be determined for the above Stefan-Maxwell equations (1 through 3). These parameters were solved for using the data of Okada and coworkers[10] and a nonlinear regression analysis on four macroscopic transport properties, namely the ionic conductivity, the proton transference number, the water electro-osmotic coefficient and the water permeability [11]. From this analysis, $\mathcal{D}_{H^+,K^+}$ is set to a large arbitrary value ($1 \cdot 10^6$

m^2/s) based on fitting the experimental data the best. For the other $\mathcal{D}_{ij}$'s, a linear dependence of $\ln(\mathcal{D}_{ij})$ with the proton fraction in the membrane y_{HM} is assumed

$$\mathcal{D}_{ij} = \mathcal{D}_{ij}^{\dagger} \exp\left(m_{ij}(y_{\mathrm{HM}} - y_{\mathrm{HM}}^{\dagger})\right) \tag{17}$$

where $y_{\mathrm{HM}}^{\dagger}$ is either equal to 0 or 1 whether $\mathcal{D}_{ij}^{\dagger}$ refers to the membrane in K^+ or H^+ form, respectively. The values of the m_{ij} and $\mathcal{D}_{ij}^{\dagger}$ coefficients are given in Table I.

Boundary conditions.— To study the contaminant-ion effect, a hydrogen-pump setup is simulated where a membrane with a defined concentration of contaminating ion is placed in between two platinum electrodes that are in equilibrium with a water reservoir. In this analysis, for simplification, it is assumed that there is a set concentration of potassium ions, which cannot leave or enter the membrane system (they have a zero flux). As a boundary condition, the K^+ concentration is set at one electrode and a zero K^+ flux is set at the other one. Alternatively, an integral equation can be used where the total K^+ concentration is set ; both approaches yield the same results. At both electrodes, the equilibrium relationship between H_2O in the membrane and H_2O in contact with the membrane is used. For liquid or dilute solutions conditions (thus assuming that water activity is close to unity), an empirical polynomial relationship between the water content in the membrane λ and the fraction of protons y_{HM} was deduced from the experimental data reported by Okada *et al.*[10]

$$\lambda = \frac{x_{\mathrm{H_2O}}}{x_{\mathrm{M^-}}} = -3.9578 y_{\mathrm{HM}}{}^4 + 8.5846 y_{\mathrm{HM}}{}^3 - 10.087 y_{\mathrm{HM}}{}^2 + 13.526 y_{\mathrm{HM}} + 13.227 \tag{18}$$

To solve for the membrane thickness, two boundary conditions are for equations 11 and 12: η is set to 0 at one side of the membrane and at the other side, it is related to the membrane thickness using the relationship

$$\eta \approx \frac{l_{\mathrm{dry,\,H^+\,form}}{}^3}{\bar{V}_{\mathrm{HM}} l^2} \tag{19}$$

where an isotropic expansion / contraction of the membrane has been assumed, $l_{\text{dry, H}^+\text{ form}}$ is the thickness of a dry membrane in the proton form, and $\bar{V}_{\text{HM}}$ is the partial molar volume of HM, and is given in Table I.

Finally, the current density is set, which translates into a proton flux given by Faraday's law,

$$\mathbf{N}_{\text{H}^+} = \frac{\mathbf{i}}{F} \tag{20}$$

To determine the cell potential for the given current density, kinetic equations are used at each electrode, with an arbitrary reference potential of 0 V being set at the anode in the solid phase (Φ_1). In this fashion, the cell potential is given as the cathode minus the anode (0 V) solid-phase potentials. The electrochemical reaction at each electrode is

$$\text{H}_2 \Leftrightarrow 2\text{H}^+ + 2\text{e}^- \tag{21}$$

for which the kinetics are expressed using a Butler-Volmer equation

$$i = aL_e i_0 \left[\frac{P_{\text{H}_2}}{P_{\text{H}_2}^{\text{ref}}} \exp\left(\frac{\alpha_a F}{RT} \left(\Phi_1 - \Phi_2 \right) \right) - \left(\frac{a_{\text{HM}}}{a_{\text{HM}}^{\text{ref}}} \right)^2 \exp\left(\frac{-\alpha_c F}{RT} \left(\Phi_1 - \Phi_2 \right) \right) \right] \tag{22}$$

where aL_e is taken to be 300 $\text{cm}^2_{\text{Pt}}/\text{cm}^2$, $\alpha_a = \alpha_c = 1$, and $i_0 = 0.3$ A/cm^2 [12], and the reference conditions are 1 bar of hydrogen and a membrane fully in its proton form. In the above expression, a_{HM} is given by $f_{\text{HM}} y_{\text{HM}}$. In using equation 22, the two-step kinetic pathway is not used [14], which may deviate the results at very low hydrogen concentrations slightly. The membrane being simulated is an 1100 equivalent-weight and the governing equations are solved numerically using BAND(j)[6] and a 25 node discretization. The hydrogen partial pressures on both electrodes are set to 1 bar.

3. **Results and Discussion**

As a first result, the limiting current density as a function of average K^+ contamination is examined, as shown in Figure 1. This limiting current density is due to the H^+ concentration becoming zero at the cathode layer and is the maximum current density that can be sustained through the membrane. From the figure, one can deduce that at low to medium cation contaminant there should not be substantial impact on performance. However, as the average concentration of K^+ increases, this effect becomes limiting in the cell. This is especially true if one considers that typical PEFC operating conditions are around 1.5 A/cm^2. In fact, such a current density could not be achieved in a membrane with a swollen thickness of 60 μm (*e.g.*, liquid-equilibrated Nafion 112) where more than half of the H^+ is substituted with K^+, unless the potassium ions had a way to move out of the membrane. The impact of thickness is relatively dramatic as seen in Figure 1, with the result that a very thin membrane can contain a significant amount of cation contamination without demonstrating appreciable changes in performance. Finally, although not shown, the impact of activity coefficients on the curves is minimal.

While Figure 1 displays the limiting current density, it is also of interest to examine the approach to this maximum value. Figure 2 gives the cell potential and normalized potential loss as a function of average relative K^+ fraction $\langle y_{\mathrm{KM}} \rangle$ for various current densities. The cell potential is for the hydrogen-pump setup. The divergence from the pure proton-form value, which is shown in Figure 2(b), can be interpreted as the minimum potential loss in a PEFC. An actual PEFC will have other losses associated with it due to oxygen dilution and diffusion, slow oxygen-reduction-reaction kinetics, drying out of the membrane at the anode side if not humidified enough, *etc*. besides just the ohmic and H^+ activity effects shown in Figure 2. In the figure, the cell potential gradually increases until an average K^+ fraction that is on the order of 70 to 80 % or so of its maximum value of $\langle y_{\mathrm{KM}} \rangle$. Beyond this value, the potential increases sharply as it should do as the limiting current is approached. In other

words, Figure 1 is a plot of the points at which the potential goes toward infinity. Figure 2 allows one to get a feel for how important contamination will be in a PEFC in terms of operating potential loss due to ohmic and H^+ activity effects. This potential loss, however, does not take into account any ohmic effect that would arise from membrane drying out at the anode, as discussed below. For reference, at 75 % of the maximum value of $\langle y_{KM} \rangle$, the potential loss is on the order of 5 to 30 mV, depending on the current density. This range also indicates that the curves will not simply collapse on one another and that the proportional loss (*i.e.*, referenced to the same percentage of the maximum $\langle y_{KM} \rangle$ value) increases with current density due to the coupled phenomena inside the membrane. While it is evident that some small contamination is allowable, anything greater than 35 % or so could represent substantial losses at appreciable current densities.

The curves in Figure 2 are somewhat a function of the value of the exponent on the proton activity in equation 19. While the curves will show a similar shape for different values, the curves become more slanted and increase faster as the exponent is increased (not shown), which is not surprising since one is multiplying fractional values together. The exact value of this exponent is not necessarily known; however, it should be noted that it could be as high as four for oxygen reduction in a PEFC from overall stoichiometry. Thus, the maximum amount of contamination may be lower than that interpreted from Figure 2, although the limiting current densities will remain the same, since they are insensitive to the exponent value.

While Figures 1 and 2 demonstrate the practical limitations and effects of K^+ contamination, it is also of interest to examine the potential and H^+ profiles. Figure 3 shows these profiles for the case of 50 % average K^+ fractional contamination and for two different current densities. From the proton-fraction curves, it is clear as to how the limiting current arises by the proton concentration going to zero at the cathode even though the average

concentration is much higher. The two current densities are chosen to be one that is far and one that is close to the limiting current density (see Figure 2). It is clear that, as one approaches the limiting current density, the profile becomes more nonlinear. Unlike the proton-fraction profiles, the potential profiles remain mainly linear as the current density is increased. This means that the cross-coefficients have minimal impact and that the conductivity does not vary abruptly.

Finally, the net water flux per proton flux (i.e., proportional to the current density) in the membrane, β, is plotted as a function of $\langle y_{KM} \rangle$ for various current densities in figure 4. A value of 2.92 is observed regardless of the current density value for a pure proton membrane, which is close to that observed in the literature for the electro-osmtic coefficient for a liquid-equilibrated membrane [10, 15]. In this simulation, the water back-flux is not significant since both sides of the membrane are in contact with a unit water-activity reservoir and water is not being generated as it would in a PEFC.

When the average potassium ion fraction is increased, β increases as well and eventually reaches a maximum for a $\langle y_{KM} \rangle$ value that depends on the current density, after which it decreases until a limiting current density is attained. The maximum values for β range from 3.14 for the lowest current density (0.01 A/cm^2) to 3.23 (1.5 A/cm^2) for the highest. A value as low as 2.8 is observed for β at a value of $\langle y_{KM} \rangle$ close to unity at the lowest current density.

This is significantly different from the value of electro-osmotic coefficient of nearly 5 reported for a membrane in potassium form [10], which is explained by the fact that the water flux in the system is associated with proton and not potassium-ion movement. Overall, the β values do not vary by more that 11 % in the range of current densities investigated, which

should not be really problematic with regard to water management (e.g. drying of the anode and flooding of the cathode).

Overall, the simulations show that around 30 to 40 % contamination has no substantial impact on performance for a variety of current densities depending on the membrane thickness. This result implies that cation contamination is probably not a major concern for typically operating fuel cells. However, there are some caveats to the analysis presented above. These include the assumptions of fully humidified gas streams, isothermal conditions (room temperature), no transfer of K^+ out of the membrane, and also the use of a Nafion 1100 equivalent-weight membrane. Finally, the results presented are for steady-state operation and are not indicative of the approach to steady state and any transient effects which may occur due to the dynamic movement of the contaminant cation.

4. **Summary**

Concentrated solution theory, based on the Stefan-Maxwell multicomponent transport equations, was successfully applied to describe the transport phenomena in an ion-exchange membrane containing two cations, namely, H^+ and K^+. A generic mathematical model of the transport phenomena in the membrane was developed, and specific boundary conditions were provided for case of a hydrogen-pump setup to understand the effect of the contaminant cation on performance. The model was used to calculate limiting current densities in terms of average K^+ fraction, and shows that the maximum allowable fraction before appreciable effects on polarization is around 30 to 40 % for an 1100 equivalent-weight Nafion, although it depends on the membrane thickness and operating current density, with less impact on thinner membranes and at lower current densities.

5. Acknowledgements

The authors would like to thank helpful discussions with Bryan Pivovar and Brian Kienitz. This work was supported by the Director, Office of Science, of the U.S. Department of Energy under Contract No. DE-AC02-05CH11231.

6. List of Symbols

Nomenclature

a_i	activity of component *i*
aL_e	catalyst surface area per geometric area, m_{Pt}^2/m^2
b	constant used in the expression of the activity coefficient of a regular solution, J/mol
c_i	molar concentration, mol/m^3
c_T	total molar concentration of species, mol/m^3
$\mathcal{D}_{ij}$	diffusion coefficient for interaction between species *i* and *j*, m^2/s
$\mathcal{D}_{ij}^{\dagger}$	diffusion coefficient for interaction between species *i* and *j* in a membrane with a single cation, m^2/s
f_i	activity coefficient of component *i* in a regular mixture
F	Faraday's constant, 96487 C/mol
i	current density, A/m^2
i_0	exchange current density for hydrogen oxidation/reduction, A/m^2
l	membrane thickness, m
$l_{\text{dry, H}^+\text{ form}}$	membrane thickness of a dry membrane in the H^+ form, m
m_{ij}	slope of $\ln(D_{ij}) = f(y_{HM})$
N_i	flux density of species *i*, $mol/m^2.s$
p	pressure, Pa
R	universal gas constant, 8.3143 J/mol·K
T	absolute temperature, K
$\overline{V_i}$	partial molar volume of component *i*, m^3/mol
x	distance in the membrane from the interface between the membrane and the

	aqueous solution, m
x_i	mole fraction of species *i*
y_i	number of moles of species *i* (*i* = H^+ or K^+) divided by the total number of moles of cations in the membrane
$\langle y_i \rangle$	Average y_i in the membrane

Greek

α_a, α_c	charge transfer coefficients
β	net water flux per cation flux in the membrane
Φ	electric potential, V
η	number of moles of membrane per surface area of membrane, mol/m^2
λ	number of moles of water per mole of membrane
μ_i	(electro)chemical potential of species or component *i*, J/mol

Superscript/Subscript

†	variable related to a single-cation membrane
1	solid or electron-conducting phase
2	membrane or ion-conducting phase
C	diffusion coefficient for interaction between species *i* and *j* calculated from a membrane in the C^+ form (with C^+ = H^+ or K^+), m^2/s
ref	reference electrode conditions

References

[1] T. Okada, J. Electronanal. Chem., 465 (1999) 1.

[2] T. Okada, J. Electronanal. Chem., 465 (1999) 18.

[3] X. Cheng, Z. Shi, N. Glass, L. Zhang, J.J. Zhang, D.T. Song, Z.S. Liu, H.J. Wang, J. Shen, J. Power Sources, 165 (2007) 739.

[4] R.M. Darling, J.P. Meyers, J. Electrochem. Soc., 152 (2005) A242.

[5] B. Kienitz, H. Baskaran, T. Zawodzinski, and B. Pivovar, ECS Transactions, 11(1), 777 (2007).

[6] J. Newman, K.E. Thomas-Alyea, Electrochemical Systems, John Wiley & Sons, Inc., NJ, 2004.

[7] P.N. Pintauro, D.N. Bennion, Ind. Eng. Chem. Fundam., 23 (1984) 230.

[8] T.F. Fuller, Solid Polymer Electrolyte Fuel Cells, University of California, Berkeley, CA, 1992.

[9] J.P. Meyers, Simulation and Analysis of the Direct Methanol Fuel Cell, University of California, Berkeley, CA, 1998.

[10] T. Okada, H. Satou, M. Okuno, M. Yuasa, Journal of Physical Chemistry B, 106 (2002) 1267.

[11] C. Delacourt and J. Newman, J. Electrochem. Soc. (2008), accepted.

[12] K.C. Neyerlin, W.B. Gu, J. Jorne, H.A. Gasteiger, J. Electrochem. Soc., 154 (2007) B631.

[13] K.S. Førland, T. Okada, S.K. Ratkje, Journal of Electrochemical Society, 140 (1993) 634.

[14] J.X. Wang, T.E. Springer, R.R. Adzic, J. Electrochem. Soc., 153 (2006) A1732.

[15] T. A. Zawodzinski, Jr., T. E. Springer, J. Davey, R. Jestel, C. Lopez, J. Valerio, and S. Gottesfeld, *J. Electrochem. Soc.*, **140**, 1981 (1993).

Captions

Table I: Values of $\mathcal{D}_{ij}^{0}$ and $\overline{V_i}$ for the potassium- and proton-membrane forms and m_{ij} (slope of $\ln(\mathcal{D}_{ij}) = f(y_{HM})$) regressed from the data of Okada *et al.*[10] at T = 25°C and p = 1 atm.

Figure 1 Limiting current density as a function of the average relative fraction of potassium cations and average swollen membrane thickness for a 1100 equivalent weight membrane.

Figure 2 Cell potential (a) and normalized potential loss (b) as a function of the average relative fraction of potassium cations in a Nafion 112 membrane for various current densities.

Figure 3 Electrolyte potential (bottom curves) and relative fraction of protons (top curves) as a function of membrane position at two different current densities for a Nafion 112 membrane with an average relative fraction of potassium cations of 50 %.

Figure 4 Water flux parameter β as a function of the average potassium ion fraction in the membrane for various current densities. The dashed line represents β values for the corresponding limiting current densities.

Table I: Values of $\mathcal{D}_{ij}^{0}$ for the potassium- and proton-membrane forms and m_{ij} (slope of $\ln(\mathcal{D}_{ij}) = f(y_{HM})$) regressed from the data of Okada *et al.*[10] at T = 25°C and p = 1 atm.

m_{H^+,H_2O}	0.22	
m_{H^+,M^-}	–2.2	
m_{K^+,H_2O}	4.5	
m_{K^+,M^-}	–2.3	
m_{H_2O,M^-}	0.54	
	K-form	H-form
$\mathcal{D}^{\dagger}_{C^+,H_2O}$ (cm^2/s)	9.96x10^{-6}	6.28x10^{-5}
$\mathcal{D}^{\dagger}_{C^+,M^-}$ (cm^2/s)	1.28x10^{-6}	5.95x10^{-6}
$(\mathcal{D}^{\dagger}_{H_2O,M^-})_C$ (cm^2/s)	5.80x10^{-6}	9.96x10^{-6}
$\overline{V}_i$ (cm^3/mol)	533	553

m_{H_2O,M^-} is expressed as $m_{H_2O,M^-} = \ln\left(\mathcal{D}^{\dagger}_{H_2O,M^-}\right)_H - \ln\left(\mathcal{D}^{\dagger}_{H_2O,M^-}\right)_K$. No m_{ij} is defined for H^+,K^+ since $\mathcal{D}_{H^+,K^+}$ is set to a very high constant value. Values of m_{ij}'s for the four remaining $\mathcal{D}_{i,j}$'s were refined by a least-square nonlinear regression of four measured transport properties reported in [10]. See reference [11] for a more in-depth explanation of the regression.

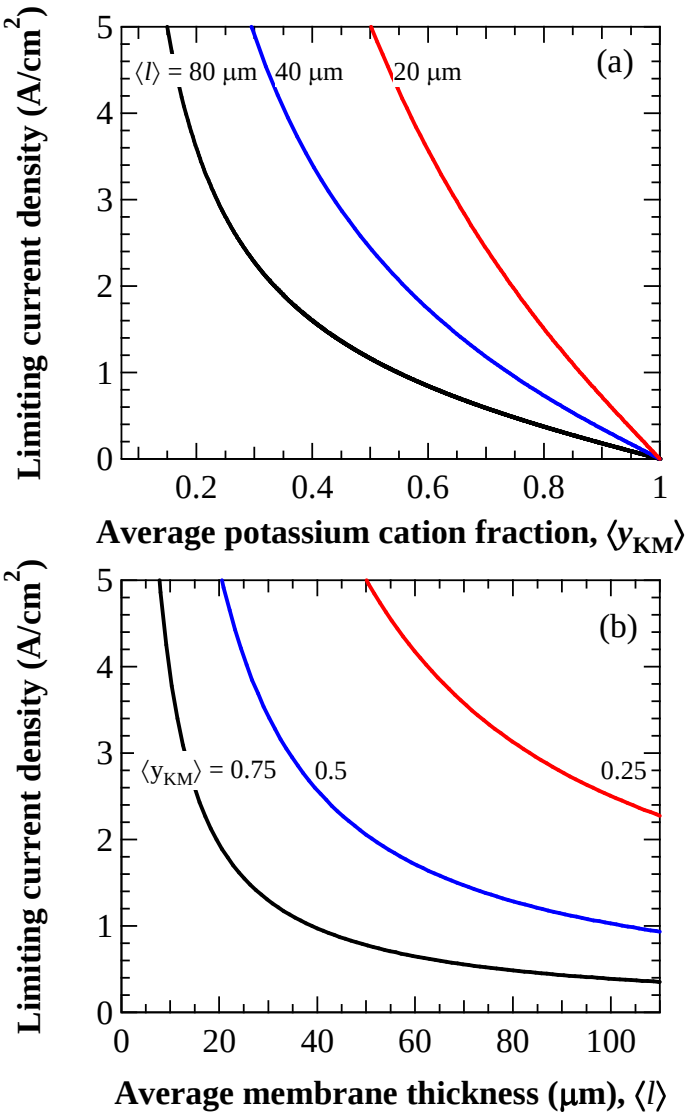

Figure 1 Limiting current density as a function of the average relative fraction of potassium cations and average swollen membrane thickness for a 1100 equivalent weight membrane.

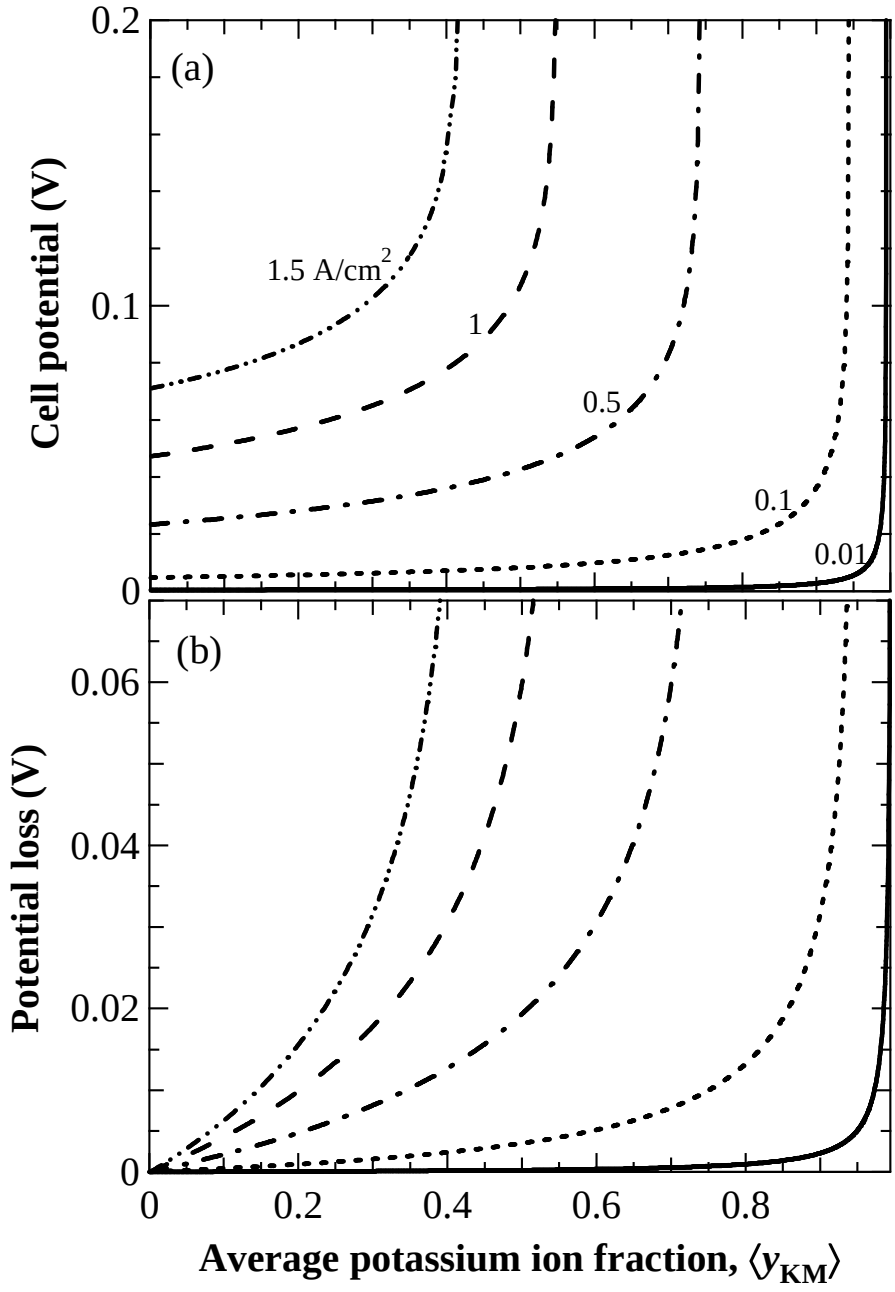

Figure 2 Cell potential (a) and normalized potential loss (b) as a function of the average relative fraction of potassium cations in a Nafion 112 membrane for various current densities.

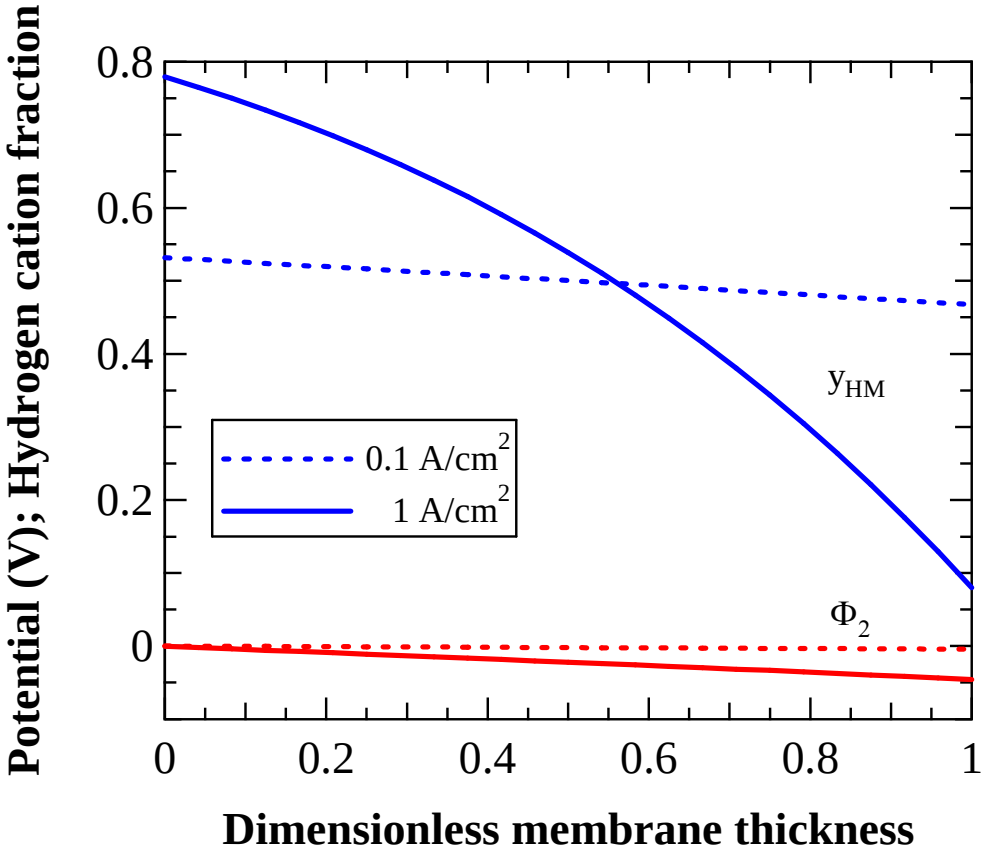

Figure 3 Electrolyte potential (bottom curves) and relative fraction of protons (top curves) as a function of membrane position at two different current densities for a Nafion 112 membrane with an average relative fraction of potassium cations of 50 %.

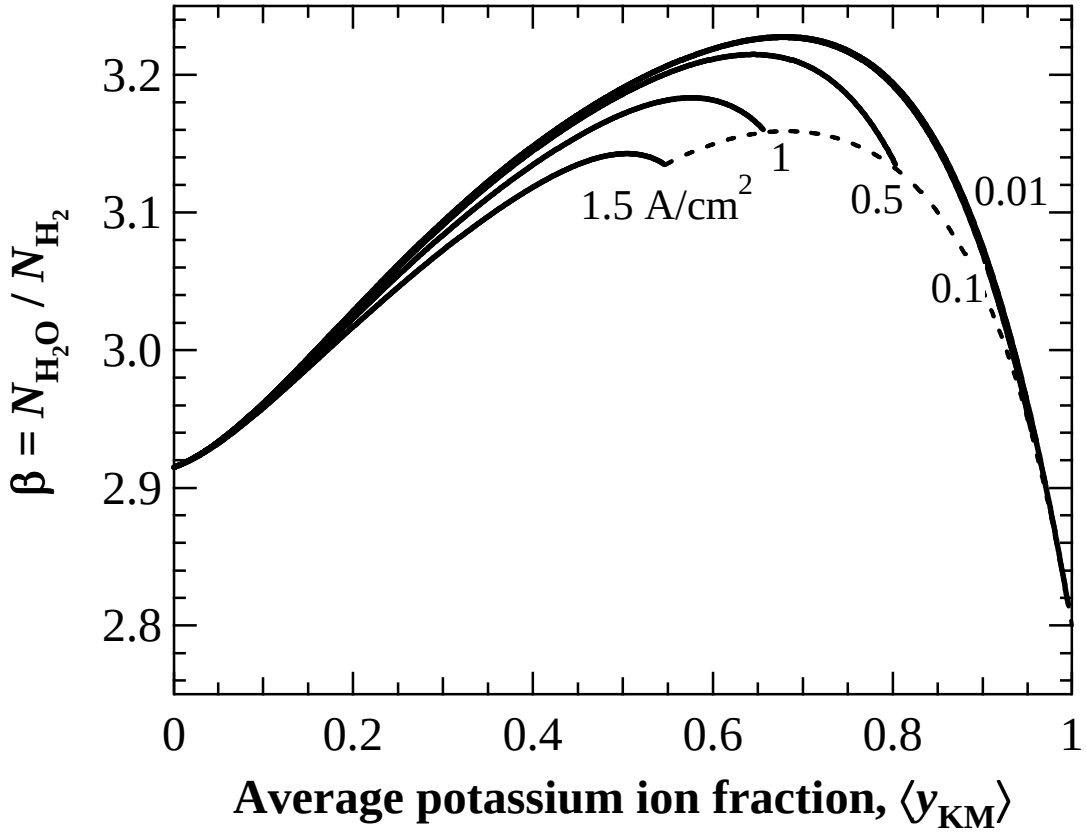

Figure 4 Water flux parameter β as a function of the average potassium ion fraction in the membrane for various current densities. The dashed line represents β values for the corresponding limiting current densities.